Environmental Technology & Innovation 20 (2020) 101083

Contents lists available at ScienceDirect

Environmental Technology & Innovation

journal homepage: www.elsevier.com/locate/eti

Acetic acid extraction from rumen fluid by forward osmosis

Jamshed Ali Khan [a], Luong N. Nguyen [a], Hung C. Duong [a,b], Long D. Nghiem [a,c,*]

[a] Centre for Technology in Water and Wastewater, University of Technology Sydney, Ultimo NSW 2007, Australia
[b] Le Quy Don Technical University, Hanoi, Viet Nam
[c] NTT Institute of Hi-Technology, Nguyen Tat Thanh University, Ho Chi Minh City, Viet Nam

ARTICLE INFO

Article history:
Received 13 June 2020
Received in revised form 31 July 2020
Accepted 31 July 2020
Available online 5 August 2020

Keywords:
Forward osmosis
Rumen fluid
Volatile fatty acids
Acetic acid
Extraction
Lignocellulosic biomass

ABSTRACT

This study evaluated the potential of extracting acetic acid from rumen fluid by forward osmosis (FO). Unlike other FO applications to extract water and reduce the feed water volume, this research used FO to mimic the ruminant intestines for extracting acetic acid from rumen fluid to a clean matrix with a minimum water flux. The FO extraction of acetic acid was optimised with a synthetic solution using cellulose triacetate (CTA) and thin film composite (TFC) polyamide membranes under different operating parameters (e.g. membrane orientation and stripping solution pH). Under the same operating conditions the CTA membrane showed higher acetic acid transport than the TFC polyamide membrane. Increasing the stripping solution pH from 5.5–6.5 to 9.0–10.0 increased the acetic acid transport through both CTA and TFC membranes. On the other hand, the membrane orientation had no discernible effect on the transport of acetic acid. Under the optimum conditions, the FO process using the CTA membrane exhibited negligible water flux and extracted 27% of the maximum attainable acetic acid from the synthetic solution within 8 h of operation. The optimised conditions were used to elaborate the FO extraction of acetic acid from a real rumen fluid. Considerably lower extraction rate from the real rumen fluid was observed compared to the synthetic solution, suggesting the need for further research to address the complexity of the rumen matrix.

1. Introduction

Ruminant animals such as cows, sheep, and koalas have a unique digestive system that allows them to acquire nutrients and energy from a plant-based (lignocellulose) diet. Their stomach consists of four compartments instead of one like in other animals. The first compartment, often called the fore-stomach or rumen, contains a complex microbial community of bacteria, archaea, fungi, and protozoa to break down cellulosic materials under anaerobic conditions (Creevey et al., 2014; Yue et al., 2013). The breaking down of cellulosic material leads to the formation of rumen fluid mainly composed of phospholipids, amino acids, inorganic ions, dicarboxylic acids, gases, carbohydrate, glycerides, cholesterol esters, and volatile fatty acids (VFAs) (Artegoitia et al., 2017). Amongst these constituents, VFAs are vital as they provide energy and nutrient for ruminant animals after diffusing through their intestine (Yue et al., 2013). In other words, the unique microbes in the rumen convert lignocellulosic biomass that is indigestible by other animals to beneficial VFAs. This unique capacity of ruminant animals has spurred scientific interests to mimic their rumen for producing VFAs from lignocellulosic biomass such as crop residues and other lignocellulosic waste (Nguyen et al., 2020a).

* Correspondence to: School of Civil and Environmental Engineering, Faculty of Engineering and Information Technology, The University of Technology Sydney, 15 Broadway, Ultimo NWS 2007, Australia.
E-mail address: duclong.nghiem@uts.edu.au (L.D. Nghiem).

https://doi.org/10.1016/j.eti.2020.101083
2352-1864/

VFAs production from lignocellulosic biomass might play an important role in industrial development in coming years. VFAs are valuable biochemicals that can replace petroleum-based chemicals for the production of pharmaceuticals, plastics, and other products of the modern economy (Makinde and Sonaiya, 2010; Roy et al., 2013). Each year, about 150 billion metric tons of lignocellulosic biomass is generated, mostly as a by-product from agriculture and forestry activities (Balat and Ayar, 2005). Therefore, VFAs production from lignocellulosic biomass in engineered rumen reactors can obviate the current dependence on crude oil and other fossil resources for raw chemicals. A major technical challenge in the design and development of engineered rumen reactors is the extraction of VFAs from the rumen fermented broth (i.e. commonly known as rumen fluid) like the process inside the ruminant animals' intestine. In this context, we propose forward osmosis (FO) to mimic the ruminant intestine for extracting VFAs from rumen fluid in engineered rumen reactors. The aim is to promote the realisation of VFAs production from lignocellulosic biomass.

FO has emerged as a versatile technology platform for treatment of various impaired waters that are deemed challenging to other treatment processes. Unlike the pressure-driven membrane processes (e.g. nanofiltration and reverse osmosis), FO does not require an externally applied hydraulic pressure but harnesses the intrinsic osmotic gradient between two solutions to facilitate the transport of water and/or solute across the membrane (Khan et al., 2019). Driven by the osmotic gradient, the FO process embodies several superior attributes such as low membrane fouling, fouling reversibility, and simple operation. Given these notable attributes, the FO process has been demonstrated for a wide range of applications including wastewater treatment (Fujioka et al., 2018; Nguyen et al., 2020b; Zheng et al., 2019), phosphorus recovery from wastewater and digested sludge (Ansari et al., 2016; Nguyen et al., 2016; Vu et al., 2019), water recovery from drilling mud (Chen et al., 2015; Hickenbottom et al., 2013), and food processing (An et al., 2019; Kim et al., 2019). Most of these FO applications involve the dewatering of the less concentrated feed solution by the high concentrated draw solution with a focus on increasing the water flux and reducing the reverse solute flux.

In this study, the FO process was harnessed to promote the extraction of acetic acid from rumen fluid prior to its enrichment and utilisation. In other FO applications, water is extracted from the feed to the draw solution under the osmotic gradient caused by the difference in the feed and draw solution concentrations. Despite the high selectivity of the FO membrane, water flux always coincides with the reverse transport of solute from the draw solution to the feed. Unlike water, which permeates through the membrane from a low concentrated solution to a high concentrated solution, the solutes permeate through the membrane in the opposite direction i.e. from a high concentrated solution to a low concentrated solution following the natural concentration gradient. This solute transport or the reverse solute flux has been dealt as a major impediment in the development of FO technology and many attempts have been made to mitigate it (Hancock and Cath, 2009; Suh and Lee, 2013; Zhao and Zou, 2011). This study, however, aimed at using the transport of solute through the FO membrane as a means to promote the extraction of acetic acid from rumen fluid while maintaining minimum or no water flux. The negligible hydraulic pressure and the minimum water flux applied might render the FO process resistant to the high fouling propensity of the rumen fluid that might be a serious challenge to other pressure-driven membrane processes.

Given the abovementioned purpose, this study systematically examined the influence of membrane type, membrane orientation, pH of the stripping solution, and the rumen matrix on the acetic acid extraction by the FO process. The broader idea was to develop an engineered rumen reactor to produce VFAs from lignocellulosic biomass and then extract the produced VFAs from fermented solution by FO.

2. Materials and methods

2.1. The FO system and the feed and stripping solutions

The lab-scale FO system used in this study consisted of a membrane module, two gear pumps, two flow metres, and two beakers for feed and stripping solutions (Fig. 1). The membrane module had a flat-sheet FO membrane coupon sandwiched between two identical and symmetrical acrylic semi-cells having a flow channel with length, width, and depth of 7.6, 2.6, and 0.3 cm, respectively. The effective area of the membrane was 19.76 cm^2. Two gear pumps (Cole-Parmer, 75211-15) were used to circulate the feed and stripping solution, while two acrylic flow metres (Cole-Parmer, 32461-42) were placed before the inlets of the FO membrane module to measure the feed and stripping solution flow rates. The feed beaker was placed on a digital balance (Adam Equipment, PGL 8001) connected to a computer to allow for the record of change in the solution beaker mass after every 60 min. The pH of the feed and the stripping solution was measured every hour using two pH metres (Hach, HQ40d).

Two types of non-commercial FO membranes including thin film composite (TFC) polyamide and cellulose triacetate (CTA) were used in this study. The TFC polyamide membrane is a proprietary FO membrane from Hydration Technology Innovation (Albany, OR), while the CTA membrane is from Fluid Technology Solutions Inc., USA. The TFC polyamide membrane is fabricated via interfacial polymerisation having a thin polyamide active layer with a porous polysulfone support layer. The CTA membrane is prepared from cellulose triacetate along with an embedded support layer using the phase inversion method. The pore sizes of the CTA and TFC membrane are in the range of 0.29–0.30 nm. These two membranes were selected for their contrasting properties in terms of fouling resistance, water permeability, and particularly reverse solute flux. Recent results suggest that the CTA FO membrane is less susceptible to fouling but exhibits lower water permeability and higher reverse solute flux than the TFC polyamide one (Fam et al., 2013; Ong et al., 2012;

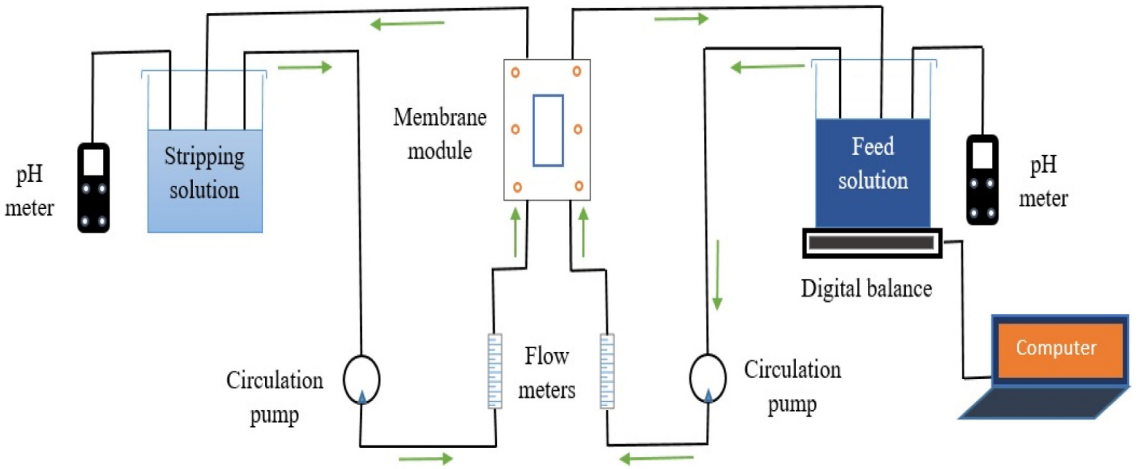

Fig. 1. Schematic diagram of the lab-scale FO system.

Wang et al., 2016). Therefore, it was necessary to elucidate the effect of these two membranes with different reverse solute flux on the FO extraction of acetic acid from rumen fluid.

A synthetic solution and real rumen fluid were used as feed solutions in this study. The synthetic acetic acid 50 mM solution was prepared by dissolving lab-grade acetic acid (>99% purity from Sigma-Aldrich) in deionised (DI) water. This low acetic acid concentration was deliberately selected to minimise the water flux while ensuring sufficient transport rate of acetic acid through the FO membrane. DI water was used as the stripping solution to capture acetic acid transferred through the FO membrane from the feed. Rumen fluid from a twelve years old fistulated cow was also used to replicate the real rumen matrix. Coarse matter in the rumen fluid was removed by straining it through a two-layered cheesecloth followed by a two-layered mesh filter (Nguyen et al., 2019). The obtained rumen fluid was kept at 4 ° C in the dark before the extraction experiment. The rumen fluid contains acetic acid as one of the main VFAs but we could not analyse the rumen fluid to find its acetic acid concentration. Therefore, synthetic acetic acid was added to the rumen fluid to obtain a concentration of at least 50 mM.

2.2. Analytical methods

The concentration of acetate ions in the stripping solution was analysed using an Ion Chromatography system (Thermo Scientific, Dionex Integrion RFIC) with an anionic column (Dionex IonPac^{TM} AS15). NaOH 38 mM solution was used as the eluent. The stripping solution samples (i.e. 1 mL each) were collected every hour during the FO acetic acid extraction experiments. A calibration curve was obtained using a series of standard acetic acid solution concentrations of 0.5, 2.0, 5.0, 7.5, and 10.0 mM with the linear regression coefficient R^2 of 0.994. Each sample took 30 min to develop a chromatogram. The peak curve for acetate ions appeared between 7 and 8 min in each chromatogram. It is necessary to note that with the NaOH 38 mM eluent, all acetic acid in the stripping solution is conversed to acetate ions.

2.3. Experimental protocol

2.3.1. Characterisation of FO membranes

Membrane transport characteristics including the pure water permeability coefficient (A), salt permeability coefficient (B), and structure parameters were determined using the standard protocol described in the previous studies (Cath et al., 2013; Luo et al., 2018). A and B values were determined by a cross-flow RO system using DI water and a NaCl 34 mM respectively as the feed (Luo et al., 2016). The RO system was stabilised for at least one hour at the transmembrane pressure (ΔP) of 10 bar and a cross-flow velocity (CFV) of 25 cm/s before the water flux (i.e. J_{RO} for the process with DI water feed and J_{NaCl} with the NaCl solution feed) was recorded. To determine the B value, feed and permeate samples were collected to determine the observed NaCl rejection (R_{ob}). The A and B values were determined as (Luo et al., 2016):

$$A = \frac{J_{RO}}{\Delta P} \tag{1}$$

$$B = J_{NaCl}\left(\frac{1 - R_{ob}}{R_{ob}}\right) exp\left(-\frac{J_{NaCl}}{k_f}\right) \tag{2}$$

Table 1
Key transport parameters of the CTA and TFC polyamide FO membranes.

Parameters	CTA	TFC
Pure water permeability — A value (L/m^{2}hbar)	0.84	2.10
NaCl permeability — B value (m/s)	8.96×10^{-8}	1.96×10^{-8}
Structural parameter — S value (mm)	0.58	0.30

where k_f was the mass transfer coefficient of the cross-flow RO membrane cell. k_f was calculated using the salt concentration at the membrane surface with the thin-film theory for concentration polarisation:

$$k_f = \frac{J_{\mathrm{NaCl}}}{ln\left[\frac{\Delta P}{\pi_b - \pi_p}\left(1 - \frac{J_{\mathrm{NaCl}}}{J_{RO}}\right)\right]} \tag{3}$$

In Eq. (3), π_b and π_p were the feed and permeate osmotic pressures and can be determined by their corresponding salt concentrations according to the van't Hoff equation.

The membrane structural parameter (S) determines the degree of internal concentration polarisation (ICP). The S value is defined as below (Luo et al., 2016):

$$S = \frac{l\tau}{\varepsilon} \tag{4}$$

where l is thickness of the supporting layer, τ is tortuosity of the supporting layer, and ε is porosity of the supporting layer.

Here, the S value was experimentally determined using the cross-flow FO system mentioned above with NaCl 0.5 M as the draw solution and clean water as the feed solution. The membrane active layer was in contact with the feed solution. The FO system was stabilised for one hour before recording the water flux (J_{FO}) to determine the S value using (Cath et al., 2013; Luo et al., 2016):

$$S = \frac{D_s}{J_{FO}} ln\left(\frac{B + A\pi_{D,b}}{B + J_{FO} + A\pi_{F,m}}\right) \tag{5}$$

In Eq. (5), D_s is the bulk solution diffusivity of the draw solute, $\pi_{D,b}$ is the bulk osmotic pressure of the draw solution, and $\pi_{F,m}$ is the osmotic pressure at the membrane surface on the feed side.

2.3.2. FO extraction of the acetic acid from the synthetic solution and rumen fluid

All experiments were carried out using a lab-scale FO system for at least 8 h at room temperature (25 ± 1 °C). The volumes of feed solution and stripping solution were 2.0 L. The CFV of both the feed and stripping solution was constant at 10.6 cm/s with a co-current configuration. An aliquot sample (1 mL) was taken from stripping solution every hour for acetate ions concentration analysis.

Two ranges of stripping solution pH were applied in this study to assess the impact of stripping solution pH on the acetic acid transport across the FO membrane. One was the pH range of DI water (5.5–6.5) and the other was pH of 9.0–10.0 achieved by adding 0.2 mL of NaOH 0.1 M solution to the stripping solution after every 8–10 min.

3. Results and discussions

3.1. Membrane characterisation

The membrane characterisation results allow for the comparison between the CTA and TFC polyamide membranes with respect to mass transfer across the membrane. Consistent with the literature, the CTA membrane exhibited a lower water permeability (A) but significantly higher salt permeability (B) and structural parameter (S) than the TFC polyamide membrane under the same testing conditions (Table 1). It is noteworthy that while the water permeability of the CTA membrane was only one fourth of that of the TFC polyamide membrane, its salt permeability was 4.5-fold higher than the salt permeability achieved by the TFC polyamide membrane. The markedly high salt permeability/water permeability ratio of the CTA membrane might favour the extraction of acetic acid with minimised water flux from the rumen fluid during the FO process compared to the TFC polyamide one.

3.2. Acetic acid extraction from the synthetic solution

In the FO process with the synthetic solution feed, the impacts of membrane fouling and complex feed compositions on the transport of acetic acid through the membrane could be excluded, allowing for the accurate evaluation of the influences of FO membrane properties and process operating conditions on the acetic acid extraction. The experimental results shown in Fig. 2 confirmed the advantage of the CTA membrane over the TFC polyamide membrane with respect to

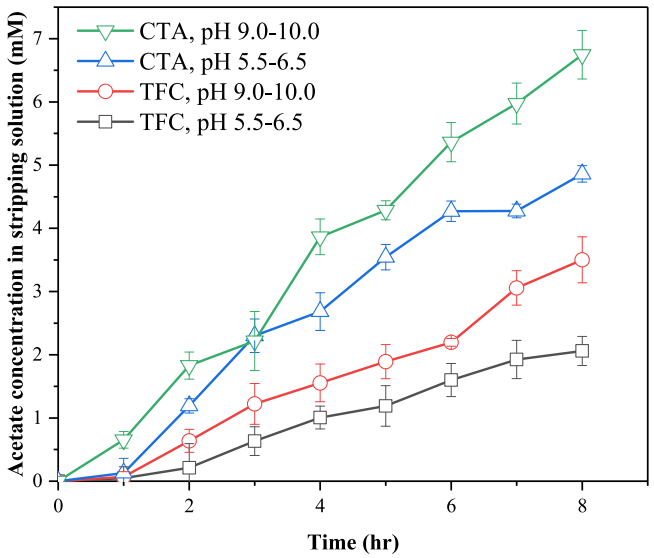

Fig. 2. Effect of membrane and pH on acetic acid permeation. Experimental conditions were as follows: acetic acid 50 mM solution feed, membrane active layer facing feed solution, feed and stripping solution CFV = 10.6 cm/s. The error bars represent standard deviation of data obtained from two independent experiments.

the extraction of acetic acid. Under the same operating conditions (e.g. membrane orientation and stripping solution pH), the acid acetic extraction rate of the FO process with the CTA membrane was higher than the TFC polyamide membrane, demonstrated by its higher acetate ions concentration in the stripping solution at the same operating time (Fig. 2). The higher acetic acid extraction rate of the CTA compared with the TFC polyamide membrane was consistent with its higher salt permeability reported in Section 3.1. Indeed, previous studies have demonstrated that the CTA membrane exhibits lower salt rejection and higher reverse salt flux than the TFC polyamide membrane (Luo et al., 2018; Madsen et al., 2015).

It is noteworthy that the membrane pore sizes might not be the prominent factor affecting the transport of acetic acid through the FO membranes. The CTA and TFC membranes used in this study have pore sizes in the range of 0.29–0.30 nm while the calculated molecular diameter of acetic acid molecule is approximately 0.45 nm. The diffusion of acetic acid through the FO membrane might be controlled by the Donnan effect, not the size exclusion. Indeed, a recent study has found that the electrostatic interaction between the solute molecules and the membrane rather than the size of solute molecules affects the transport of solutes through the membrane (Zheng et al., 2019).

Moreover, the transport of acetic acid through the membranes during the FO process of the synthetic solution feed was primarily driven by the acid concentration difference between the feed and the stripping solution. This is demonstrated by the discrepancy in the acetic acid transport rate through the membranes when the stripping solution pH was elevated from 5.5–6.5 to 9.0–10.0. At the elevated stripping solution pH, more acetic acid was extracted from the synthetic solution through the FO membranes, leading to higher acetate ion concentration measured in the stripping solution (Fig. 2). It is necessary to note in both feed and stripping solutions acetic acid dissociated into negatively charged acetate ion and proton: $CH_3COOH \leftrightarrow CH_3COO^- + H^+$ (pKa = 4.76). This equilibrium strongly depended on the pH of the solutions. The synthetic solution feed was highly acidic (i.e. pH = 3); thus, acetic acid existed mainly as neutral molecules in the feed. On the other hand, 80% and almost 100% of all permeated acetic acid molecules from feed to the stripping solution existed in the form of acetate ions at pH of 5.5–6.5 and 9.0–10.0, respectively. The higher acetic acid concentration difference across the FO membranes at the stripping solution pH of 9.0–10.0 rendered more acetic acid transferred through the membranes, leading to higher measured acetate ion concentration in the stripping solution compared with that at the stripping solution pH of 5.5–6.5 (Fig. 2).

The linear relationship between the measured acetate ion concentration of the stripping solution and the operating time shown in Fig. 2 might be attributed to the excessively high acetic acid concentration of the synthetic solution feed (50 mM) compared with that of the stripping solution (i.e. <1 mM after 8 h of extraction). If the FO process with the synthetic solution feed was extended, more acetic acid from the feed would transfer to the stripping solution, hence reducing the driving force for the acetic acid extraction from the feed. The acetate ion concentration curves shown in Fig. 2 would flatten when the driving force dwindled with extended operating time. Theoretically, acetate ion concentration in the stripping solution can increase to 25 mM when the system is at equilibrium with extended operating time. Nevertheless, as demonstrated in Fig. 2, after 8 h of the FO operation, the CTA can achieve 27% and 19% of the maximum extraction potential at pH of 9.0–10.0 and of 5.5–6.5, respectively. Over the same experimental period, the TFC polyamide membrane can only achieve 14% and 8% of the maximum extraction potential at the respective pH of 9.0–10.0 and of 5.5–6.5.

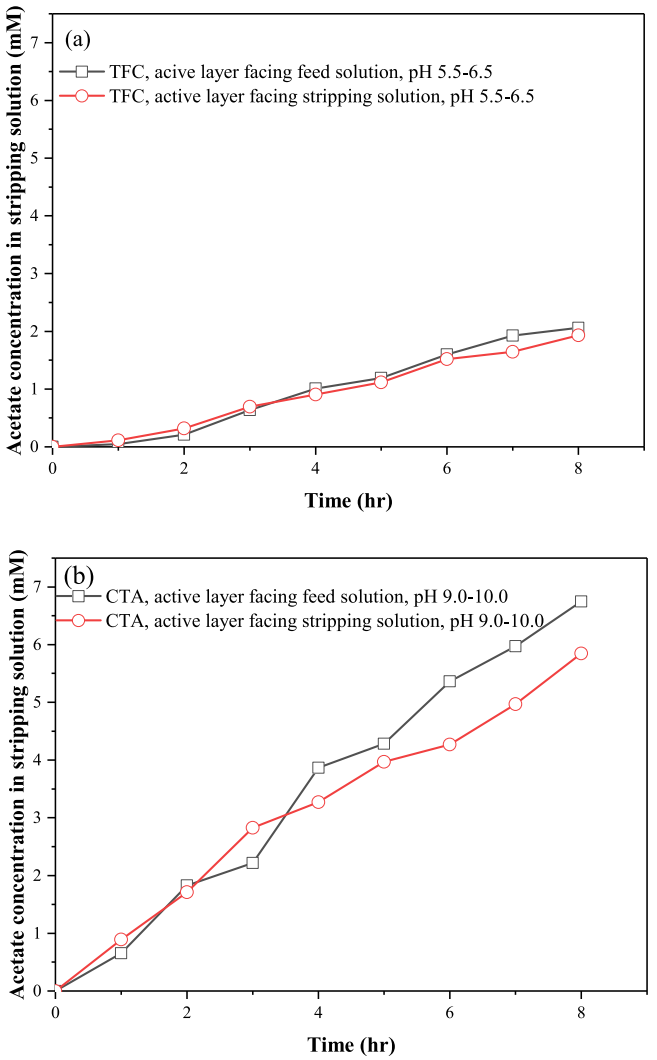

Fig. 3. Effect of membrane orientation on acetic acid permeation when (a) membrane was TFC polyamide and stripping solution pH was 5.5–6.5, and (b) membrane was CTA and stripping solution pH was 9.0–10.0. Experimental conditions were as follows: synthetic acetic acid 50 mM solution feed, feed and stripping CFV = 10.6 cm/s.

The effect of membrane orientation was evaluated for both the membranes at the selected stripping solution pH values (Fig. 3). The TFC polyamide membrane orientation had negligible effect on the acetic acid permeation to the stripping given the inbuilt feature of this membrane to hinder solutes transport across the membrane (Zhao et al., 2011). The acetate ion concentrations in the stripping solution during the FO process of the synthetic solution feed using the TFC polyamide membrane were similar when the membrane orientation was reversed (Fig. 3(a)). On the other hand, for the FO process using the CTA membrane, the stripping solution acetate ion concentration increased by 14% when the membrane active layer was facing the feed solution (6.7 mM) compared with that obtained when the membrane active layer was facing the stripping solution (5.8 mM) (Fig. 3 (b)). This slight increase could be attributed to the less ICP effect when the membrane active layer facing the feed solution than facing the stripping solution (i.e. the feed acetic acid concentration was much higher than that of the stripping solution). It is worth reminding that the CTA membrane had a higher S value than the TFC polyamide membrane (Table 1); therefore, the negative effect of ICP on the acetic acid extraction during the FO process with the CTA membrane was more severe than that with the TFC polyamide membrane. Thus, the effect of membrane orientation on the acetic acid extraction rate was more noticeable for the CTA compared to the TFC polyamide membrane (Fig. 3).

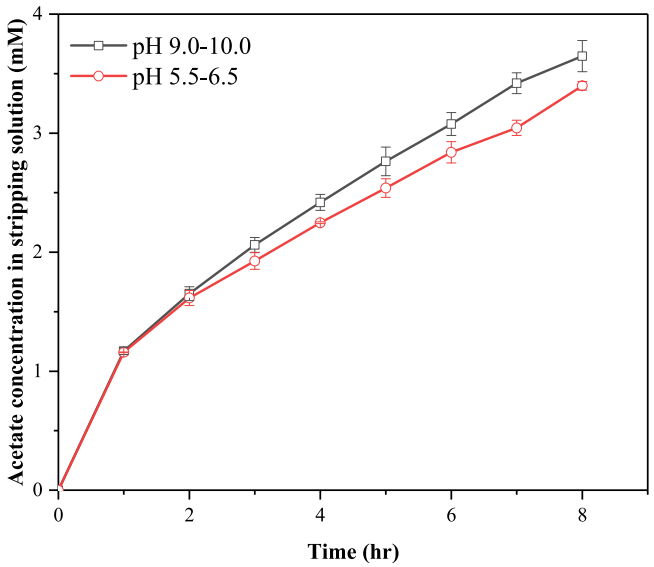

Fig. 4. Acetic acid permeation from a rumen fluid at two different pH values. Experimental conditions were as follows: rumen fluid with acetic acid 50 mM as the feed, CTA membrane, membrane active layer facing feed solution, feed and stripping CFV = 10.6 cm/s. The error bars represent standard deviation of data obtained from two independent experiments.

3.3. Acetic acid extraction from rumen fluid

The FO process using the CTA membrane with the active layer facing the feed solution was used to evaluate the acetic acid extraction potential from the real rumen fluid at two stripping solution pH values (Fig. 4). The acetate ion concentration in the stripping solution increased gradually at both of the stripping solution pH values. A maximum of 3.65 mM acetate ion concentration in the stripping solution was observed after 8 h of the experiment which is equivalent to ∼15% of the maximum attainable concentration (25 mM). In comparison, after 8 h, acetic acid extraction from the synthetic solution was 27% of the maximum attainable concentration.

The lower acetic acid extraction potential of the FO process with the real rumen fluid compared to the synthetic solution could be attributed to the complex nature of the rumen fluid that could lead to membrane fouling. The real rumen fluid contained various constituents including phospholipids, inorganic ions, amino acids, dicarboxylic acids, volatile and non-volatile fatty acids, glycerides, carbohydrate, and cholesterol esters (Artegoitia et al., 2017). These constituents hinder the flow of acetic acid from rumen fluid to the stripping solution. They also act as a source of possible transportation of other small solutes across the membrane, thus creating competition for acetic acid molecules and significantly reducing the effective osmotic pressure across the membrane.

Unlike the FO process with the synthetic solution feed, in case of real rumen fluid feed, the stripping solution pH exerted indiscernible influence on the acetic acid transport across the membrane. The acetate ions concentration increased from 3.40 mM to only 3.65 mM when the stripping solution pH was elevated from 5.5–6.5 to 9.0–10.0. It can be due to the high pH (∼5.6) of the rumen fluid feed. At this pH value, approximately 80% of the acetic acid molecules were in the form of acetate ions and only the remaining 20% acetic acid molecules were available for transport across the membrane. Therefore, even when the stripping solution pH was increased from 5.5–6.5 to 9.0–10.0, the increase in acetate ion concentration in the stripping solution was unnoticeable due to the limited availability of acetic acid molecules in the feed solution. This is consistent with the lower acetic acid extraction potential of the FO process with the real rumen fluid compared to the synthetic solution feed as discussed above.

3.4. Water transfer between the feed and stripping solutions

Water flux from the stripping to the feed solution was measured by monitoring the changing weight of the feed solution. Negligible water flux was observed when either the synthetic solution or the real rumen fluid was used as the feed (Fig. 5). The type of membranes, membrane orientation, and the stripping solution pH showed indiscernible effect on water flux. For the synthetic solution, water flux was highest (i.e. 1) at the beginning of the experiment, then gradually decreased towards zero with the operating time. These results were expected due to the low transmembrane osmotic pressure gradient generated by a small difference in acetic acid concentrations between the feed and stripping solution (<50 mM).

When rumen fluid was used as the feed solution, the water flux from the stripping solution to the feed solution was more noticeable at around 3 L/m^{2}h. The higher water flux observed with the rumen fluid feed could be attributed to

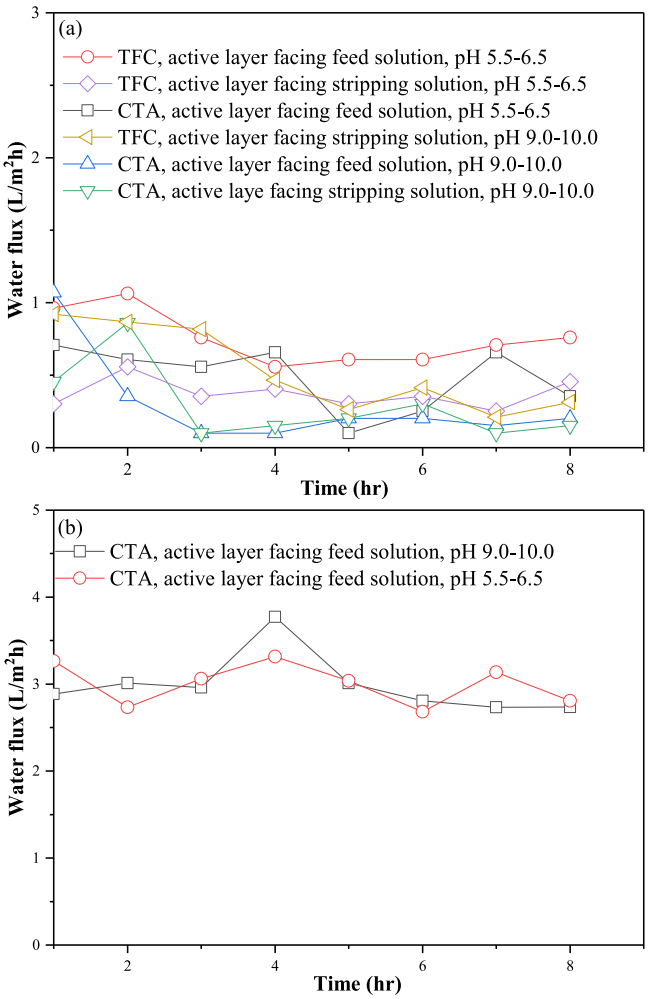

Fig. 5. Changes in water flux as a function of extraction time when (a) the synthetic acetic acid 50 mM solution and (b) rumen fluid with acetic acid 50 mM was used as the feed.

the increased transmembrane osmotic pressure gradient because of the high concentration of the rumen fluid. Besides acetic acid (>50 mM), the real rumen fluid contained other solutes and hence offered a higher osmotic pressure than the synthetic acetic acid 50 mM solution. As a result, the driving force for water transport from the stripping solution to the rumen fluid feed was higher than that to the synthetic solution feed.

3.5. The pH of feed and stripping solution

Changes in pH of the feed and stripping solutions were recorded after every hour of each experiment. pH values of the synthetic solution and rumen fluid remained constant during all FO experiments (Fig. 6). Both feed solutions acted as the bulk solution for acetic acid and therefore the continuous outflow of acetic acid molecules into the stripping solution did not alter the acidic environment of the feed solutions. The initial and final pH values (∼5.7) for rumen fluid was much higher than those for the synthetic solution (∼3.0). The higher pH value of rumen fluid could be explained by the presence of organic solutes and inorganic ions resulting in a high buffering capacity.

Unlike the feed solution pH, a notable decrease of the stripping solution pH was observed at the beginning of all extraction experiments (Fig. 7). The observed pH decrease was attributed to the influx of acetic acid from the feed solution. The pH drop was more significant in the first hour and became gradual in the remaining seven hours of the experiments.

4. Conclusions

This study provides preliminary but new insight into the potential of acetic acid extraction from the rumen fluid by FO. The membrane characterisations showed better separation performance by the TFC polyamide membrane in terms

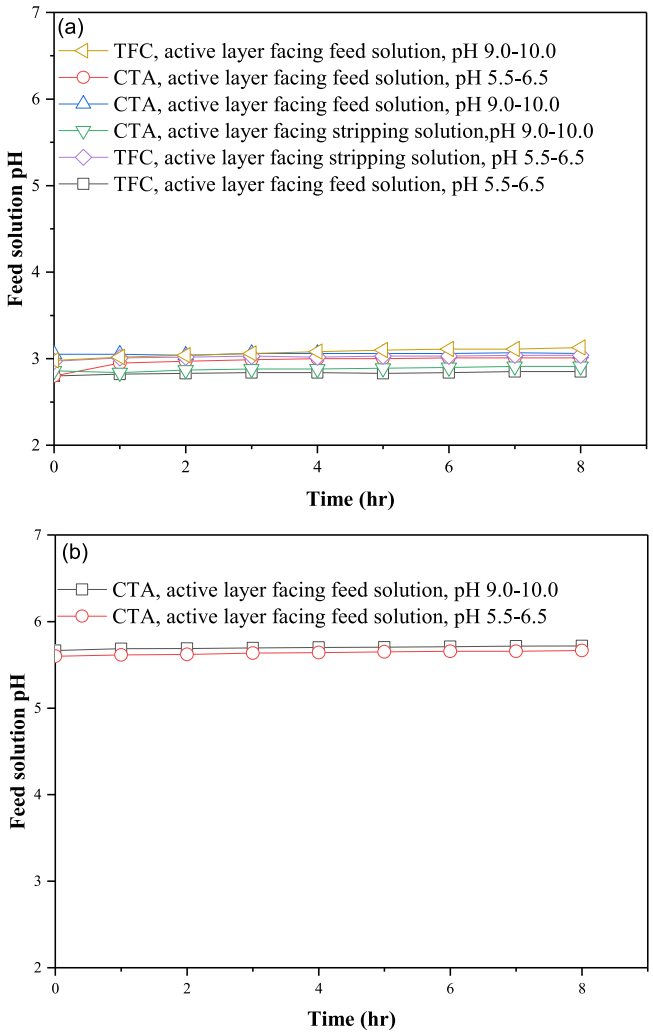

Fig. 6. Changes in feed solution pH as a function of extraction time when (a) the acetic acid 50 mM solution and (b) rumen fluid with acetic acid 50 mM was used as the feed.

of pure water permeability, solute rejection, and structural parameter compared to the CTA membrane. However, the CTA membrane allowed more acetic acid transport through the membrane than the TFC polyamide one under the same experimental conditions. Moreover, the acetic acid transport through the membrane increased as the stripping solution pH was elevated from 5.5–6.5 to pH 9.0–10.0 for both membranes. The effect of membrane orientation on acetic acid transport was insignificant for both TFC polyamide and CTA membranes. The highest acetic acid permeation to stripping solution was achieved with the CTA membrane having the active layer facing the feed solution and at the stripping solution pH of 9.0–10.0. The optimised condition was used to evaluate the extraction of acetic acid from the real rumen fluid. Considerably lower acetic acid extraction rate was observed compared to the synthetic solution. Thus, further work is required to improve the extraction rate in a realistic condition involving the complex rumen fluid matrix.

CRediT authorship contribution statement

Jamshed Ali Khan: Data curation, Writing - original draft. **Luong N. Nguyen:** Supervision, Methodology, Writing - review & editing. **Hung C. Duong:** Methodology, Writing - review & editing. **Long D. Nghiem:** Conceptualization, Methodology, Supervision, Writing - review & editing.

Declaration of competing interest

The authors declare that they have no known competing financial interests or personal relationships that could have appeared to influence the work reported in this paper.

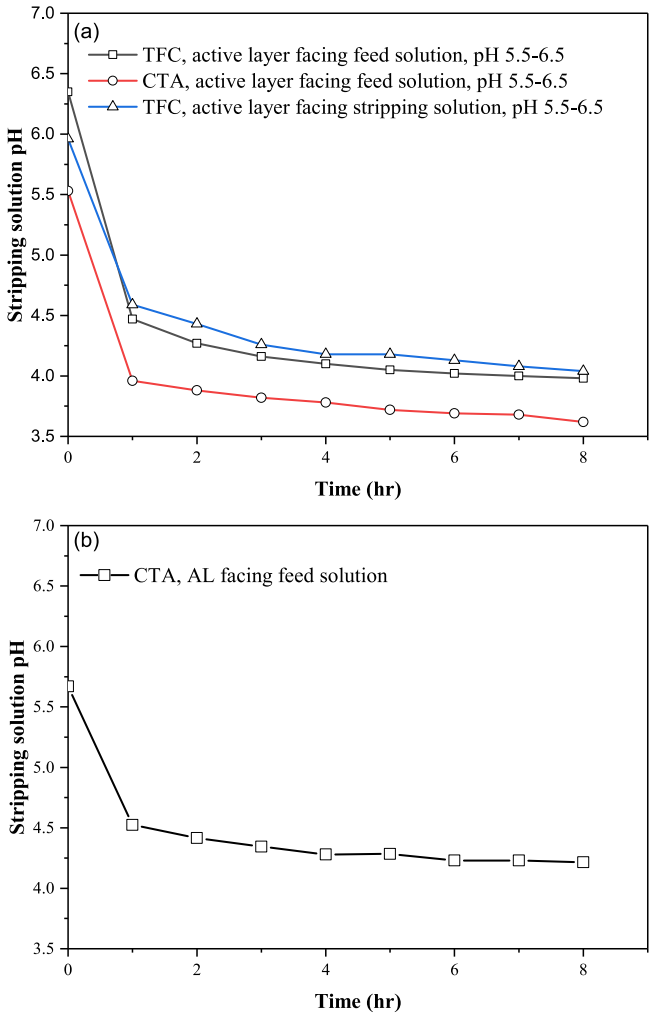

Fig. 7. Changes in stripping solution pH as a function of extraction time when (a) acetic acid 50 mM solution (b) rumen fluid with acetic acid 50 mM was used as the feed.

References

An, X., Hu, Y., Wang, N., Zhou, Z., Liu, Z., 2019. Continuous juice concentration by integrating forward osmosis with membrane distillation using potassium sorbate preservative as a draw solute. J. Membr. Sci. 573, 192–199.

Ansari, A.J., Hai, F.I., Price, W.E., Nghiem, L.D., 2016. Phosphorus recovery from digested sludge centrate using seawater-driven forward osmosis. Sep. Purif. Technol. 163, 1–7.

Artegoitia, V.M., Foote, A.P., Lewis, R.M., Freetly, H.C., 2017. Rumen fluid metabolomics analysis associated with feed efficiency on crossbred steers. Sci. Rep. 7 (1), 2864.

Balat, M., Ayar, G., 2005. Biomass energy in the world, use of biomass and potential trends. Energy Sour. 27 (10), 931–940.

Cath, T.Y., Elimelech, M., McCutcheon, J.R., McGinnis, R.L., Achilli, A., Anastasio, D., Brady, A.R., Childress, A.E., Farr, I.V., Hancock, N.T., Lampi, J., Nghiem, L.D., Xie, M., Yip, N.Y., 2013. Standard methodology for evaluating membrane performance in osmotically driven membrane processes. Desalination 312, 31–38.

Chen, G., Wang, Z., Nghiem, L.D., Li, X.-M., Xie, M., Zhao, B., Zhang, M., Song, J., He, T., 2015. Treatment of shale gas drilling flowback fluids (SGDFs) by forward osmosis: Membrane fouling and mitigation. Desalination 366, 113–120.

Creevey, C.J., Kelly, W.J., Henderson, G., Leahy, S.C., 2014. Determining the culturability of the rumen bacterial microbiome. Microb. Biotechnol. 7 (5), 467–479.

Fam, W., Phuntsho, S., Lee, J.H., Shon, H.K., 2013. Performance comparison of thin-film composite forward osmosis membranes. Desalin. Water Treat. 51 (31–33), 6274–6280.

Fujioka, T., Nguyen, K.H., Hoang, A.T., Ueyama, T., Yasui, H., Terashima, M., Nghiem, L.D., 2018. Biofouling mitigation by chloramination during forward osmosis filtration of wastewater. Int. J. Environ. Res. Public Health 15 (10), 2124.

Hancock, N.T., Cath, T.Y., 2009. Solute coupled diffusion in osmotically driven membrane processes. Environ. Sci. Technol. 43 (17), 6769–6775.

Hickenbottom, K.L., Hancock, N.T., Hutchings, N.R., Appleton, E.W., Beaudry, E.G., Xu, P., Cath, T.Y., 2013. Forward osmosis treatment of drilling mud and fracturing wastewater from oil and gas operations. Desalination 312, 60–66.

Khan, J.A., Shon, H.K., Nghiem, L.D., 2019. From the laboratory to full-scale applications of forward osmosis: Research challenges and opportunities. Curr. Pollut. Rep. 5 (4), 337–352.
Kim, D.I., Gwak, G., Zhan, M., Hong, S., 2019. Sustainable dewatering of grapefruit juice through forward osmosis: Improving membrane performance, fouling control, and product quality. J. Membr. Sci. 578, 53–60.
Luo, W., Xie, M., Hai, F.I., Price, W.E., Nghiem, L.D., 2016. Biodegradation of cellulose triacetate and polyamide forward osmosis membranes in an activated sludge bioreactor: Observations and implications. J. Membr. Sci. 510, 284–292.
Luo, W., Xie, M., Song, X., Guo, W., Ngo, H.H., Zhou, J.L., Nghiem, L.D., 2018. Biomimetic aquaporin membranes for osmotic membrane bioreactors: Membrane performance and contaminant removal. Bioresour. Technol. 249, 62–68.
Madsen, H.T., Bajraktari, N., Hélix-Nielsen, C., Van der Bruggen, B., Søgaard, E.G., 2015. Use of biomimetic forward osmosis membrane for trace organics removal. J. Membr. Sci. 476, 469–474.
Makinde, O., Sonaiya, E., 2010. A simple technology for production of vegetable-carried blood or rumen fluid meals from abattoir wastes. Anim. Feed Sci. Technol. 162 (1–2), 12–19.
Nguyen, C.N., Duong, H.C., Chen, S.-S., Thi Nguyen, H., Hao Ngo, H., Guo, W., Quang Le, H., Cong Duong, C., Thuy Trang, L., Hoang Le, A., Thanh Bui, X., Dan Nguyen, P., 2020b. Water and nutrient recovery by a novel moving sponge – Anaerobic osmotic membrane bioreactor – Membrane distillation (AnOMBR-MD) closed-loop system. Bioresour. Technol. 312, 123573.
Nguyen, N.C., Nguyen, H.T., Ho, S.-T., Chen, S.-S., Ngo, H.H., Guo, W., Ray, S.S., Hsu, H.-T., 2016. Exploring high charge of phosphate as new draw solute in a forward osmosis–membrane distillation hybrid system for concentrating high-nutrient sludge. Sci. Total Environ. 557–558, 44–50.
Nguyen, L.N., Nguyen, A.Q., Johir, M.A.H., Guo, W., Ngo, H.H., Chaves, A.V., Nghiem, L.D., 2019. Application of rumen and anaerobic sludge microbes for bio harvesting from lignocellulosic biomass. Chemosphere 228, 702–708.
Nguyen, A.Q., Nguyen, L.N., Johir, M.A.H., Ngo, H.-H., Chaves, A.V., Nghiem, L.D., 2020a. Derivation of volatile fatty acid from crop residues digestion using a rumen membrane bioreactor: A feasibility study. Bioresour. Technol. 312, 123571.
Ong, R.C., Chung, T.-S., Helmer, B.J., de Wit, J.S., 2012. Novel cellulose esters for forward osmosis membranes. Ind. Eng. Chem. Res. 51 (49), 16135–16145.
Roy, M., Karmakar, S., Debsarcar, A., Sen, P.K., Mukherjee, J., 2013. Application of rural slaughterhouse waste as an organic fertilizer for pot cultivation of solanaceous vegetables in India. Int. J. Recy. Org. Waste Agricult. 2 (1), 6.
Suh, C., Lee, S., 2013. Modeling reverse draw solute flux in forward osmosis with external concentration polarization in both sides of the draw and feed solution. J. Membr. Sci. 427, 365–374.
Vu, M.T., Price, W.E., He, T., Zhang, X., Nghiem, L.D., 2019. Seawater-driven forward osmosis for pre-concentrating nutrients in digested sludge centrate. J. Environ. Manag. 247, 135–139.
Wang, X., Zhao, Y., Yuan, B., Wang, Z., Li, X., Ren, Y., 2016. Comparison of biofouling mechanisms between cellulose triacetate (CTA) and thin-film composite (TFC) polyamide forward osmosis membranes in osmotic membrane bioreactors. Bioresour. Technol. 202, 50–58.
Yue, Z.-B., Li, W.-W., Yu, H.-Q., 2013. Application of rumen microorganisms for anaerobic bioconversion of lignocellulosic biomass. Bioresour. Technol. 128, 738–744.
Zhao, S., Zou, L., 2011. Relating solution physicochemical properties to internal concentration polarization in forward osmosis. J. Membr. Sci. 379 (1), 459–467.
Zhao, S., Zou, L., Mulcahy, D., 2011. Effects of membrane orientation on process performance in forward osmosis applications. J. Membrane Sci. 382 (1–2), 308–315.
Zheng, L., Price, W.E., McDonald, J., Khan, S.J., Fujioka, T., Nghiem, L.D., 2019. New insights into the relationship between draw solution chemistry and trace organic rejection by forward osmosis. J. Membr. Sci. 587, 117184.